Excited-state intramolecular relaxation of the lipophilic probe 12-(9-anthroyloxy)stearic acid

ARTICLE *in* THE JOURNAL OF PHYSICAL CHEMISTRY · JULY 1991

DOI: 10.1021/j100167a023

3 AUTHORS, INCLUDING:

Mario N Berberan Santos
University of Lisbon
200 PUBLICATIONS **3,366** CITATIONS
SEE PROFILE

Manuel Prieto
University of Lisbon
177 PUBLICATIONS **4,479** CITATIONS
SEE PROFILE

Excited-State Intramolecular Relaxation of the Lipophilic Probe 12-(9-Anthroyloxy)stearic Acid

M. N. Berberan-Santos,* M. J. E. Prieto,

Centro de Química-Física Molecular, Instituto Superior Técnico, 1096 Lisboa Codex, Portugal

and A. G. Szabo

Institute for Biological Sciences, National Research Council of Canada, Ottawa, Ontario, Canada K1A 0R6
(Received: May 17, 1990; In Final Form: February 1, 1991)

Multiexponential and emission wavelength dependent decays of fluorescence were observed for the 12-(9-anthroyloxy)stearic acid in hydrocarbon solvents. This behavior is attributed to the intramolecular rotational relaxation of the fluorophore in agreement with Matayoshi and Kleinfeld (*Biophys. J.* **1981**, *35*, 215). The dependence of steady-state anisotropies on the emission wavelength is rationalized on the basis of a simple model (isotropic rotor with wavelength-dependent decay).

Introduction

The ester derivatives of 9-anthroic acid, namely the *n*-(9-anthroyloxy)stearic acid series (*n*-AS, *n* = 2, 3, 6, 7, 9, 10, 12), have been used extensively in the study of molecular assemblies such as micelles and membranes.[1-5]

The photophysics of 9-anthroic esters was studied by Werner and co-workers in a series of papers.[6-8] They showed that the ground state of this fluorophore is nonplanar due to the steric hindrance between the carboxy group and the ring peri hydrogens. Electronic delocalization in the S_1 state (which has strong charge-transfer character) counteracts this effect, and the emissive relaxed state has a more planar geometry (see Figure 1). The effect of the alkyl substituent on the excited-state rotation was also noted by Werner and Hercules,[6,9] who showed that *tert*-butyl 9-anthroate does not attain the "planar" configuration in rigid media, while this was still able to occur with methyl 9-anthroate, which has a much smaller ester group. This was recently confirmed by Al-Hassan and El-Bayoumi.[10] The first evidence for a correlation between excited-state rotation rate and solvent viscosity was presented by Matayoshi and Kleinfeld.[11] Their work, partly based on low-precision phase-modulation data, was largely overlooked. A viscosity effect on the rotation rate was also reported for the corresponding ketones.[12] Excited-state barrierless relaxation was observed for several dyes in the picosecond time scale.[13] As will be shown, the present molecule shows analogous behavior, but on a longer time scale and with the important difference that relaxation occurs through a continuum of emitting states.

Since several authors report single-exponential decays for the *n*-AS probes in viscous media,[14-18] at variance with the above, we have decided to reconsider the problem and further characterize the photophysics of these probes. The typical member 12-AS was selected for a first study.

Materials and Methods

Chemicals. USP mineral light (L) and heavy (H) oils were free of fluorescent impurities. Methylcyclohexane (MCH) from Merck was of spectroscopic grade. Octadecyl 9-anthroate (9-OA) and 12-(9-anthroyloxy)stearic acid (12-AS) were obtained from Molecular Probes (Eugene, OR), and their purity was checked by TLC. Methyl 9-anthroate (9-MeA) was synthesized by standard procedures (acid chloride and alcohol) and 6-(9-anthroyloxy)undecane (6-AU) according to the procedure of Parish and Stock.[19] Triton X-100 from BDH was scintillation grade, and sodium dodecyl sulfate (SDS) from Merck (p.a.) were used without further purification. All other chemicals were of the highest purity commercially available.

Steady-State Measurements. The steady-state fluorescence spectra and anisotropies were measured with either a Perkin-Elmer MPF-3 spectrofluorometer or a Perkin-Elmer MPF-44A spectrofluorometer. Spectra were corrected by using a calibration curve obtained from fluorescence standards[20] (MPF-3) or using a DCSU 2 spectral correction unit (MPF-44A). Sample temperature was controlled to within 0.2 °C. Band-passes were set to 3-4 nm, in both excitation and emission.

The emission anisotropies were measured by use of HNP'B UV-transmitting dichroic film polarizers (Polaroid Corp., Inc.).

Time-Resolved Measurements. The fluorescence decays were recorded with a Spectra Physics mode-locked synchronously pumped and cavity dumped dye laser system whose output was frequency doubled with a KDP crystal to give excitation pulses with a pulse width of 20 ps at a repetition rate of 825 kHz. The fluorescence was detected by a Hamamatsu 1564 U microchannel plate after passing through a polarizer set at the magic angle and a Jobin Yvon H10 monochromator (4-nm band-passes). The electronic components were those usually employed in time-correlated single-photon counting.[21] The experiments were performed using a resolution of 42 ps/channel and 1024 channels in the multichannel analyzer. A total of 10000 counts were accumulated in the maximum channel. The excitation wavelength was 305 nm. Temperature was controlled to within 0.2 °C. The fluorescence decay parameters were obtained after convolution analysis using the Marquardt algorithm, a background signal being always

(1) Waggoner, A. S.; Stryer, L. *Proc. Natl. Acad. Sci. U.S.A.* **1970**, *67*, 579.
(2) Thulborn, K. R.; Sawyer, W. H. *Biochim. Biophys. Acta* **1978**, *511*, 125.
(3) Blatt, E.; Sawyer, W. H. *Biochim. Biophys. Acta* **1985**, *822*, 43.
(4) Storch, J.; Kleinfeld, A. M. *Biochemistry* **1986**, *25*, 1717.
(5) Chefurka, W.; Chatelier, R. C.; Sawyer, W. H. *Biochim. Biophys. Acta* **1987**, *896*, 181.
(6) Werner, T. C.; Hercules, D. M. *J. Phys. Chem.* **1969**, *73*, 2005.
(7) Werner, T. C.; Hoffman, R. M. *J. Phys. Chem.* **1973**, *77*, 1611.
(8) Werner, T. C.; Matthews, T.; Soller, B. *J. Phys. Chem.* **1976**, *80*, 533.
(9) Werner, T. C. In *Modern Fluorescence Spectroscopy*; Wehry, E. L. Ed.; Heyden & Son: London, 1976; Vol. 2, Chapter 7, pp 302-310.
(10) Al-Hassan, K. A.; El-Bayoumi, M. A. *Chem. Phys. Lett.* **1986**, *123*, 39.
(11) Matayoshi, E. D.; Kleinfeld, A. M. *Biophys. J.* **1981**, *35*, 215.
(12) Swayambunathan, V.; Lim, E. C. *J. Phys. Chem.* **1985**, *89*, 3960.
(13) Bagchi, B.; Fleming, G. R. *J. Phys. Chem.* **1990**, *94*, 9.
(14) Thulborn, K. R.; Dilley, L. M.; Sawyer, W. H.; Treloar, F. E. *Biochim. Biophys. Acta* **1979**, *558*, 166.
(15) Blatt, E.; Ghiggino, K. P.; Sawyer, W. H. *J. Chem. Soc., Faraday Trans. 1* **1981**, *77*, 2551.
(16) Vincent, M.; de Foresta, B.; Gallay, J.; Alfsen, A. *Biochemistry* **1982**, *21*, 708.
(17) Blatt, E.; Ghiggino, K. P.; Sawyer, W. H. *J. Phys. Chem.* **1982**, *86*, 4461.
(18) Blatt, E.; Ghiggino, K. P.; Sawyer, W. H. *Chem. Phys. Lett.* **1985**, *114*, 47.
(19) Parish, R. C.; Stock, L. M. *J. Org. Chem.* **1965**, *30*, 927.
(20) Melhuish, W. H. *Appl. Opt.* **1975**, *14*, 26.
(21) Zuker, M.; Szabo, A. G.; Bramall, L.; Krajcarski, D. T.; Selinger, B. *Rev. Sci. Instrum.* **1985**, *56*, 14.

0022-3654/91/2095-5471$02.50/0

TABLE I: "Best Fit" Fluorescence Decay Parameters at Selected Emission Wavelengths for the 12-AS Probe in USP Heavy Oil at 0 °C (991 cP)[a]

λ_{em}, nm	α_1	τ_1, ns	α_2	τ_2, ns	α_3	τ_3, ns	$\bar{\tau}$,[b] ns
390	0.14	9.40	0.39	2.54	0.47	0.45	5.95
410	0.28	10.37	0.41	3.11	0.31	0.56	7.85
430	0.63	10.85	0.37	2.76			9.80
440	0.68	11.13	0.32	3.29			10.19
450	0.86	11.34	0.25	3.97	−0.11	0.17	10.68
460	0.96	11.57	0.20	5.29	−0.16	0.27	11.06
480	1.26	11.34	−0.21	0.55	−0.05	0.20	11.44
500	1.51	11.61	−0.23	1.31	−0.27	0.27	11.84
520	1.68	11.79	−0.39	1.47	−0.29	0.25	12.14
540	2.72	11.89	−0.73	1.68	−0.99	0.16	12.36
560	1.96	11.95	−0.50	1.95	−0.46	0.33	12.47

[a] Preexponential values are normalized so that $\alpha_1 + \alpha_2 + \alpha_3 = 1$. Standard errors were typically 0.01, for lifetime and preexponential terms. The RMSR for most measurements was 1.01. [b] Mean lifetime $\bar{\tau} = (\sum_i \alpha_i \tau_i^2)/\sum_i \alpha_i \tau_i$.

TABLE II: "Best Fit" Fluorescence Decay Parameters for 12-AS and 9-MeA under Varying Solvent[a] or Viscosity at Selected Wavelengths

sample	viscosity, cP	λ_{em}, nm	α_1	τ_1, ns	α_2	τ_2, ns	α_3	τ_3, ns	$\bar{\tau}$,[b] ns
12-AS	0.7	410	0.37	10.90	0.30	3.19	0.33	0.92	8.93
MCH (20 °C)		440	0.72	10.70	0.28	2.92			9.95
		540	0.90	11.40	0.29	7.05	−0.19	1.57	10.90
12-AS	30	400	0.24	10.03	0.22	1.13	0.55	0.20	8.83
L (20 °C)		440	0.88	10.51	0.12	1.48			10.33
		520	1.60	11.16	−0.60	0.58			11.37
12-AS	193	400	0.19	10.23	0.40	2.50	0.41	0.39	7.26
H (20 °C)		440	0.76	10.85	0.24	2.16			10.33
		520	1.62	11.63	−0.62	0.99			11.98
12-AS	991	400	0.22	9.93	0.43	2.95	0.35	0.56	6.96
H (0 °C)		440	0.68	11.13	0.32	3.29			10.19
		520	1.68	11.79	−0.39	1.47	−0.29	0.25	12.14
9-MeA	0.7	400	1	13.00					13.00
MCH (20 °C)		440	1	12.98					12.98
		470	1	12.97					12.97
9-MeA	193	400	0.72	12.49	0.28	0.56			12.28
H (20 °C)		440	0.95	12.65	0.05	1.47			12.58
		470	1.00	12.65					12.65

[a] Solvents used were light (L) and heavy (H) USP mineral oils and methylcyclohexane (MCH). [b] $\bar{\tau} = (\sum_i \alpha_i \tau_i^2)/\sum_i \alpha_i \tau_i$.

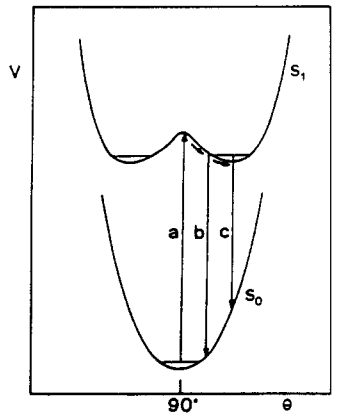

Figure 1. Ground- and excited-state potential energy curves for the 9-anthroate esters (schematic). Absorption occurs mainly in the twisted configuration (a). Emission occurs from partially (b) or totally (c) relaxed configurations. θ is the interplanar angle between the anthracene ring and the carboxy group.

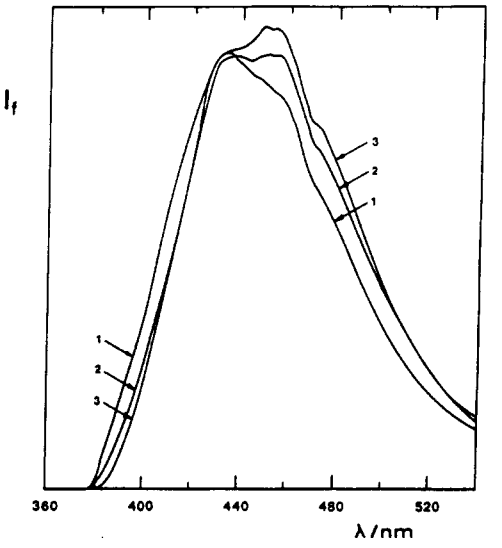

Figure 2. Steady-state fluorescence (corrected spectra) of 12-AS at three different viscosities: 991 cP (USP heavy oil at 0 °C, curve 1), 95 cP (USP light oil at 0 °C, curve 2), and 1.1 cP (MCH at −6 °C, curve 3).

subtracted prior to deconvolution. The adequacy of the fit to the decay data was determined by the inspection of the weighted residual plots, the autocorrelation of residuals, and the root mean sum of weighted squares of residuals (RMSR).[22]

Samples. The oil solutions were prepared by mixing a concentrated stock solution in MCH/ether with the oil, this solution never exceeding 0.1% (v/v) in the final mixture. Typical final concentrations were 5×10^{-5} M. (Identical results were obtained with a 5×10^{-4} M solution.) After mixing, the samples were vacuum-degassed, the ether being removed in the process. The MCH sample was degassed by the freeze–pump–thaw method (three cycles) and kept in a sealed cell. No evidence for photodecomposition was found after 30 decays. Micellar solutions were 10^{-4} M in micelles, with an average number of probes per micelle of 0.1.

Results

In Figure 2 are presented the steady-state fluorescence spectra of the 12-AS probe in hydrocarbon solvents of different viscosity and at the same temperature. An alteration of the spectral shape

(22) McKinnon, A. E.; Szabo, A. G.; Miller, D. R. *J. Phys. Chem.* **1977**, *81*, 1564.

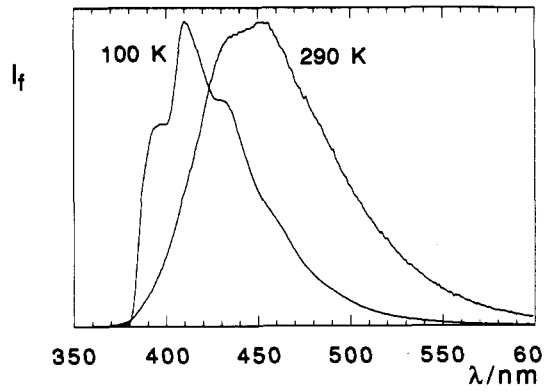

Figure 3. Steady-state fluorescence of 12-AS in ethanol–methanol (100 K) and MCH (290 K).

and a blue shift are observed with the increase of viscosity; the same results are obtained if the viscosity is altered via temperature variation (Figure 3). In contrast, for methyl 9-anthroate, minor alterations were observed, unless extreme conditions are used.

Fluorescence decays $i(\lambda,t)$ are conveniently fitted to a sum of exponentials, no physical significance being a priori attributed to the recovered lifetimes and preexponential coefficients. In most cases (see Tables I and II) the decay is well described only by a sum of three exponentials, as judged from the weighted residuals plot, autocorrelation of residuals, and root mean sum of weighted squares of residuals (RMSR). In Table I the "best fit" decay parameters at selected emission wavelengths are presented. From these data and other obtained at intermediate wavelengths the following trend is observed: at short wavelengths (390 and 410 nm), three exponentials are recovered. At an intermediate range (430–440 nm), the decay can be described by two components, but when scanning the lower energy part of the emission ($\lambda >$ 440–450 nm), again three exponentials are obtained, with one or two of the preexponential factors being negative. The mean lifetime ($\bar{\tau}$) increases in all cases when going from lower to higher wavelengths.

In Table II, a summary of results at three selected wavelengths is presented for the 12-AS probe and 9-MeA in different solvents and/or conditions. The trend observed is similar to that previously described regarding the complexity of the decays. For 12-AS the increase in mean lifetime from the blue to the red part of the emission is larger the greater the viscosity. In contrast, the decay of 9-MeA is much less viscosity dependent. Negative components are never recovered for 9-MeA in oil, and the decay is single exponential at all emission wavelengths for 9-MeA in MCH. The mean lifetime of 9-MeA is insensitive (MCH) or shows a slight increase (H, 20 °C) with increasing emission wavelength.

The previous time-dependent fluorescence data $i(\lambda,t)$, together with the steady-state emission spectra $f(\lambda)$, enable the determination of time-resolved emission spectra $F(\lambda,t)$ from[23]

$$F(\lambda,t) = f(\lambda)\, i(\lambda,t) / \int_0^\infty i(\lambda,t)\, dt \qquad (1)$$

The results for 12-AS at short and long times are presented in Figure 4.

An important time evolution of the emission spectrum is observed, with an increasing red shift as time progresses. The long time shape (>50 ns), which is essentially viscosity independent, is attained faster at lower viscosities, as observed in Figure 5; in the very low viscosity limit (Figure 5d) the different spectra are even almost superimposable.

The greater importance of emission in the lower energy region at longer times can also be appreciated from the plot of the mean lifetime vs wavelength for the different experimental conditions (Figure 6). A regular increase is observed with $\bar{\tau}$ showing a large variation from 6.0 to 12.5 ns in the case of the high-viscosity oil. When the viscosity decreases, the curves approach a flat line around 10.2 ns, as observed in Figure 6. This behavior is also

(23) Easter, J. H.; DeToma, R. P.; Brand, L. *Biophys. J.* **1976**, *16*, 571.

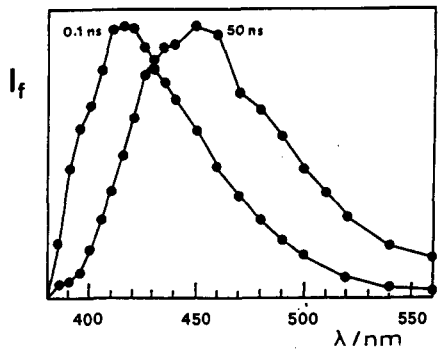

Figure 4. Time-resolved spectra of 12-AS in USP heavy oil (273 K) at early (100 ps) and late (50 ns) times.

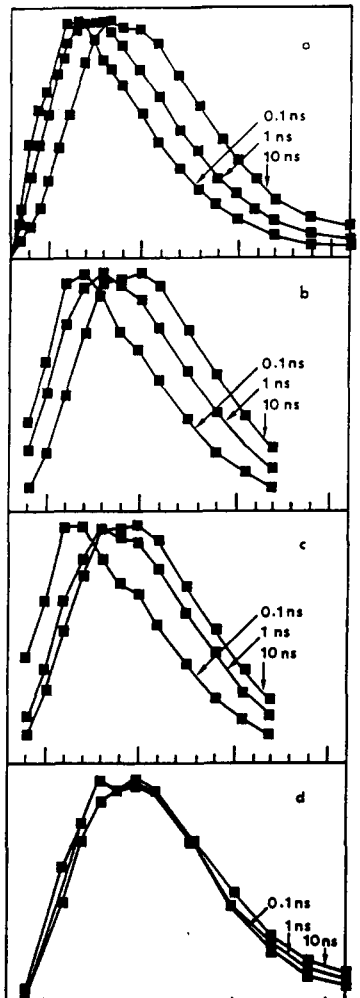

Figure 5. Time-resolved emission spectra of 12-AS in USP heavy oil at 0 °C, 991 cP (a), USP heavy oil at 20 °C, 193 cP (b), USP light oil at 20 °C, 30 cP (c), and MCH at 20 °C, 0.7 cP (d).

verified for 9-MeA with a wavelength-independent lifetime around 13.0 ns.

Preliminary results were also obtained for two other related anthroyloxy compounds, 6-(9-anthroyloxy)undecane (6-AU) and octodecyl 9-anthroate (9-OA); their mean lifetimes at three wavelengths are presented in Table III. The usual regular variation of $\bar{\tau}$ is again obtained, and when these values are compared with those in Figure 7, it can be concluded that 6-AU behavior is very similar to 12-AS, while the 9-OA compound has a lifetime variation range between those of 12-AS and 9-MeA.

Following Matayoshi and Kleinfeld,[11] steady-state anisotropies were measured in homogeneous media (Figure 7) and also in

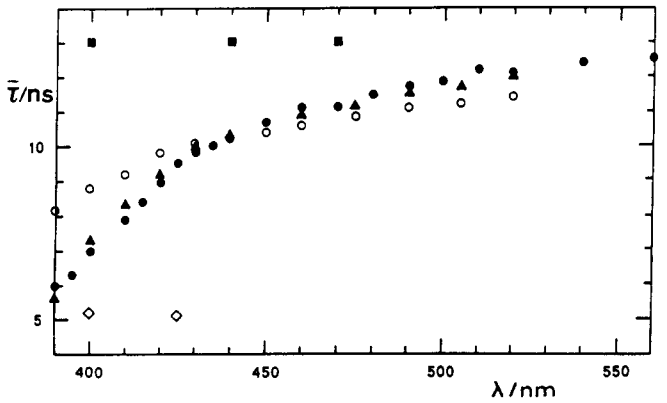

Figure 6. Mean lifetime as a function of emission wavelength: (●) 12-AS in USP heavy oil at 0 °C; (▲) 12-AS in USP heavy oil at 20 °C; (○) 12-AS in USP light oil at 20 °C; (■) methyl 9-anthroate in MCH at 20 °C (single exponential); (◇) anthracene in USP heavy oil at 20 °C (single exponential).

TABLE III: Mean Lifetimes $\bar{\tau}^a$ for 6-AU and 9-OA at Three Emission Wavelengths

sample	viscosity, cP	λ_{em}, nm	$\bar{\tau}$, ns
6-AU	133	400	9.16
H (25 °C)		450	9.85
		500	10.97
9-OA	193	400	11.38
H (20 °C)		450	11.83
		500	11.85
9-OA	991	400	10.75
H (0 °C)		450	12.10
		500	12.30

[a] Mean lifetime $\bar{\tau} = (\sum_i \alpha_i \tau_i^2)/\sum_i \alpha_i \tau_i$.

micelles (Figure 8) as a function of emission wavelength. The same trend was obtained in all cases, i.e., a decrease of the anisotropy with an increase in emission wavelength. The results in hydrocarbons show that this effect is stronger in high-viscosity conditions and that, for the same viscosity, it is much more important for 12-AS than for methyl 9-anthroate.

Discussion

Some evidence for the excited-state rotational relaxation of the 12-AS probe is already obtained from its steady-state emission in hydrocarbons of different viscosity and at constant temperature (Figure 2). The viscosity-induced blue shift of the emission and the alteration of its shape are due to a greater contribution from the "planar" conformers. The overall change could be due to viscosity-dependent Franck–Condon factors, but this explanation is ruled out by the time-resolved emission spectra (Figures 4 and 5), where a time evolution is clearly seen. The relaxation rate depends strongly on the viscosity, and in all cases the long time spectrum is essentially identical, i.e., corresponds to the same species, the "planar" conformation of the ester. This conclusion is reinforced by a comparison between the steady-state emission of 12-AS (at very high and low viscosity, Figure 3) and the 12-AS early and late spectra (Figure 5). It can be concluded that the 100-ps emission mainly originates from the nonrelaxed, "perpendicular" conformers while the 50-ns emission is due to the relaxed, "planar" conformers.

The time-dependent spectral evolution is connected with complex decays (fitted with two or three exponentials, Tables I and II). In the low-energy region of the fluorescence spectrum expected negative amplitudes are obtained, resulting from a rise time of the emission of the more planar configurations generated at longer times, while the mean lifetime shows a regular increase with wavelength (Figure 6). It is interesting to note that near the steady-state maximum intensity wavelength (440–460 nm) there is a balance in a way that the decay is almost single exponential. This fact, together with the use of wide band filters in the emission, has certainly contributed to keep hidden the complexity of the decay of these probes.

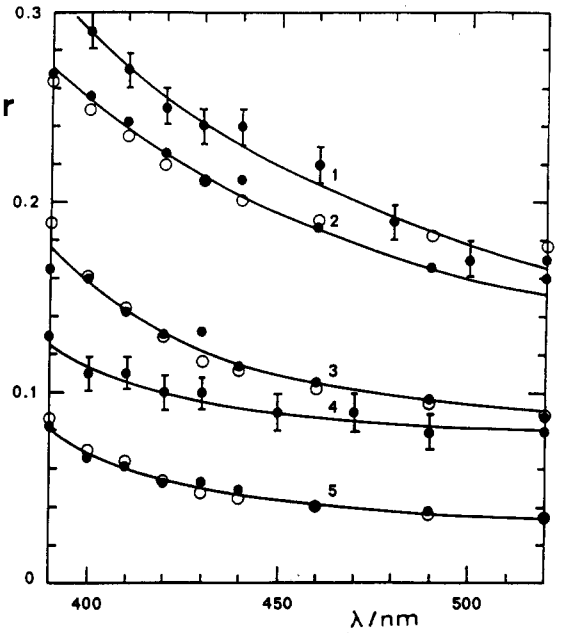

Figure 7. Fluorescence anisotropy as a function of emission wavelength (excitation wavelength 380 nm): methyl 9-anthroate in a PMMA matrix (1); 12-AS in USP heavy oil at 0 °C (2); 12-AS in USP heavy oil at 20 °C (3); methyl 9-anthroate in USP heavy oil at 0 °C (4); 12-AS in USP light oil at 20 °C (5). Open circles are the best fit values (eq 3), with rotational correlation times of 9.9 ns (2), 3.7 ns (3), and 1.2 ns (5).

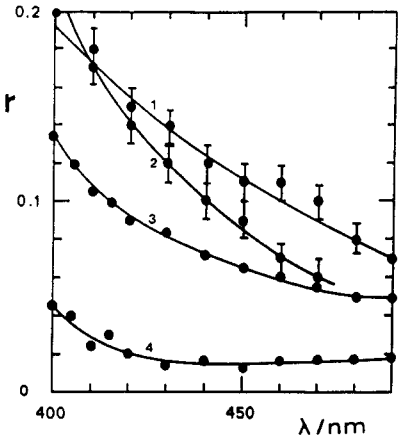

Figure 8. Fluorescence anisotropy as a function of emission wavelength (excitation wavelength 385 nm): 2-AS (1) and 12-AS (2) in Triton X-100 micelles; 2-AS (3) and 12-AS (4) in SDS micelles. Temperature was 25 °C.

The decay data show that a two-state model (twisted and "planar" conformations) cannot, in general, be applied to the present case. In fact, the decays are not even always fitted by two exponentials, showing the importance of partially relaxed conformations on the decay law. A further complicating factor is the existence of an angular distribution in the ground state, as was shown recently.[10] This distribution is associated with a low-frequency torsional mode, observed in the fluorescence spectrum of jet-cooled methyl 9-anthroate.[12,24]

Our FT-IR data also substantiate this angular distribution: the carbonyl stretching vibration of methyl 9-anthroate is unusually broad, fwhm = 16 cm^{-1} compared with a fwhm of 10 cm^{-1} of ethyl acetate and of methyl benzoate. Due to the angle dependence of the force constant, the total absorption band is the sum (over the conformers) of several narrower curves, slightly frequency shifted in their maximum.

As can be seen from Figure 6, the mean lifetime approaches anthracene's decay time (5.1 ns) near the blue edge. This also supports the notion that the blue edge emission arises mainly from

(24) Swayambunathan, V.; Lim, E. C. *J. Phys. Chem.* **1987**, *91*, 6359.

anthracene-like, almost perpendicular conformers.

On the contrary, in MCH, the mean lifetime is almost emission wavelength independent, and its average value, 10.2 ns, must be close to the decay time of the relaxed species. Given that the fluorescence quantum yields of anthracene and 12-AS in cyclohexane are respectively 0.36[25] and 0.48,[26] one can conclude that the decay time increase from 5.1 to 10.2 ns mainly results from a reduction of the nonradiative constant. Since internal conversion is a negligible process in anthracene,[27] it is the intersystem crossing efficiency ($S_1 \rightarrow T_2^8$) that is decreasing. The triplet T_2, which lies slightly below S_1 in anthracene, is less dependent on conformation than S_1; therefore, the largest stabilization of S_1 upon rotation increases the S_1–T_2 gap while a small $\Delta E(S_1$–$T_1)$ is apparently never reached.[8] The extent of coplanarity of the excited state cannot be determined from the present results, but could be higher for methyl 9-anthroate than 12-AS, as the relaxed state lifetime is higher in the first case. For methyl 9-anthroate in the gas phase, an angle of 47° was reported.[24]

The existence of a terminal acid group in 12-AS could add an extra element of complexity to its relaxation dynamics by a possible process of intramolecular quenching. In the high-viscosity media used, dynamic processes are not effective. In order to evaluate a hypothetical static contribution due to hydrogen bonding, the 6-AU compound was studied. In this case the chromophore is also attached to the central part of an aliphatic chain but without the terminal acid group, and an identical behavior to 12-AS was obtained (Table III). Interestingly, the 9-OA compound, with a terminal anthroyloxy chromophore, has a rotational relaxation behavior closer to 9-MeA, showing the importance of chain dynamics and/or bulkiness of the substituent. Another evidence that rules out the intramolecular quenching relevance are the identical trends in anisotropy (see below) observed for both 9-MeA and 12-AS. The comparison of these two molecules shows, once again, that, besides solvent friction, the nature of the alkyl group is of importance in excited-state dynamics.

The anisotropy vs wavelength profile of the 12-AS in oils depicted in Figure 7 is a consequence of the decay law dependence with wavelength, as can be shown by the use of a simple model, the isotropic rotor with a complex, wavelength-dependent decay

$$i(\lambda,t) = \sum_i \alpha_i(\lambda) \exp[-t/\tau_i(\lambda)] \quad (2)$$

for which the steady-state anisotropy is

$$r(\lambda) = r_0 \sum_i f_i(\lambda)/(1 + \tau_i(\lambda)/\tau_r) \quad (3)$$

where

$$f_i(\lambda) = \alpha_i(\lambda)\ \tau_i(\lambda)/\sum_i \alpha_i(\lambda)\ \tau_i(\lambda) \quad (4)$$

and τ_r is the rotational correlation time. The assumption of isotropic rotation for the 12-AS molecule is supported by experiment.[16] On the other hand, the fundamental anisotropy, r_0, is assumed not to change with the emission wavelength: For methyl benzoate, where the $S_2 \leftarrow S_0$ transition has a stronger charge-transfer character than $S_1 \rightarrow S_0$ emission in methyl 9-anthroate, quantum-chemical calculations by the Pariser–Parr method show that the transition dipole rotates less than 2° when going from the twisted to the planar conformation.[28] Using $r_0 = 0.4$ (excitation wavelength 380 nm), a fit was made to the curves $r = r(\lambda)$. A fair agreement between experimental and calculated anisotropies is apparent from Figure 7. The same model should explain the observed trend in micelles (Figure 8), where the decays are predictably complex and wavelength dependent.

Summary and Conclusions

The multiexponential and wavelength-dependent decays observed for the 12-AS probe in hydrocarbons have been shown to be due to the carboxy group rotation, as previously reported by Matayoshi and Kleinfeld.[11] Time-resolved spectra clearly depict the rotational relaxation dynamics and its viscosity dependence. Steady-state anisotropy variation with emission wavelength is also caused by this effect, as shown by the application of a simple model, the isotropic rotor with wavelength-dependent decay.

Acknowledgment. The authors gratefully acknowledge the expert technical assistance of Mr. D. Krajcarski with the lifetime measurements. FT-IR spectra were obtained in collaboration with J. Villalaín (Murcia University, Spain). M.B.S. is grateful to Fundação Calouste Gulbenkian (Lisbon) for a travel grant.

Registry No. *n*-AS (*n* = 12), 30536-60-8.

(25) Berlman, I. B. *Handbook of Fluorescence Spectra of Aromatic Molecules*, 2nd ed.; Academic Press: New York, 1971.
(26) Melo, E. C. C. Ph.D. Thesis, Technical University of Lisbon, 1986.
(27) Rice, J.; McDonald, D. B.; Ng, L.-K.; Yang, N. C. *J. Chem. Phys.* **1980**, *73*, 4144.
(28) Prieto, M. J. E. Ph.D. Thesis, Technical University of Lisbon, 1981.